



RESEARCH

Observer-based adaptive neural network control: the convergence properties analysis under the influence of persistent excitation level

Chujian Zeng · Ante Su · Tianrui Chen ·
Si-Zhe Chen

Received: 15 August 2024 / Accepted: 17 October 2024 / Published online: 28 October 2024
© The Author(s), under exclusive licence to Springer Nature B.V. 2024

Abstract In this paper, an observer-based adaptive neural network (NN) control method is proposed for a class of nonlinear systems. A crucial component of output feedback control is the state observer, with high gain observers widely used to estimate system states. When the system exhibits unknown dynamics, a higher gain is typically required to eliminate these effects. However, the higher gain amplifies the impact of measurement noise, thereby reducing the performance of the observer. To address this issue, we employ the adaptive high gain observer to reconstruct the system state, utilizing NNs to estimate the unknown dynamics, which allows for the selection of a relatively lower observer gain. It is noted that the convergence of the NN weights must satisfy the persistent excitation (PE) condition, which is often challenging to achieve in practice. By employing the deterministic learning method, the partial PE condition of the radial basis function NN is sat-

isfied. Furthermore, how the PE condition influences observer performance, and subsequently affects controller performance, is explored through convergence analysis in adaptive estimation. Notably, a higher PE level (the lower bound of PE) also helps mitigate the effects of measurement noise. A simulation example is provided to demonstrate the effectiveness of the proposed method.

Keywords Deterministic learning · Neural network · Adaptive high gain observer · Adaptive control · Persistent excitation condition

1 Introduction

Output feedback control methods have been extensively studied in recent decades, since the states of systems are often incompletely measurable in practice. In general, a crucial component of output feedback control is the state observer, where high gain observers are widely used to obtain the system states [1–7]. When unknown dynamics exist in the system, a higher gain is required to compensate for them. However, the higher gain may amplify the impact of measurement noise, thereby affecting the stability of the error system.

There are many methods that have been proposed to address this problem [7–11]. In [12], a unique cascade combination of extended state observers was developed that enables fast and accurate signal reconstruction while avoiding the over-amplification of measure-

C. Zeng · S.-Z. Chen
School of Automation, Guangdong University of Technology,
Guangzhou 510006, People's Republic of China

A. Su
School of Mechanical Engineering, Shandong University, Jinan
250002, People's Republic of China

T. Chen
School of Control Science and Engineering, Shandong University, Jinan, People's Republic of China

T. Chen (✉)
Center for Intelligent Medical Engineering, Shandong University, Jinan, People's Republic of China
e-mail: trchen@sdu.edu.cn

ment noise. In [13], an adaptive high gain observer (AHGO) has been proposed, where a neural network (NN) was employed to compensate for the effects of unknown dynamics. This approach allows for improved estimation accuracy for the observer while utilizing a lower gain, thereby reducing the impact of measurement noise. The development history of AHGOs can be summarized roughly as follows: In [14], an AHGO was proposed to address the issue of simultaneously estimating system states and faults, with the help of multiple-delayed systems. To relax the requirement of multiple-delayed systems, a time-varying Lyapunov function candidate was developed in [15]. In [16], a specific filter was constructed which can provide accurate parameter estimation and convergence without constructing multiple-delayed systems. In [13], by exploiting the uniformed completely observability (UCO) feature, the convergence of the developed observer was obtained.

In recent years, researchers have presented numerous adaptive output feedback control methods [17–21]. For instance, in [22], an adaptive NN control method for nonlinear systems was proposed. In [23], an adaptive neural fault-tolerant control method was developed for nonlinear systems with unmodeled dynamics and unmeasurable states. In [24], the controller design problem was investigated for non-strict-feedback systems with input delay. In [25], the issue of adaptive neural tracking control for a class of nonlinear systems with output feedback was studied.

As is well known, in the field of adaptive estimation or adaptive control, the strict persistent excitation (PE) condition needs to be satisfied in order to guarantee the convergence of NN weights or parameter estimation error [26]. Recently, Wang et al. [27] presented a deterministic learning method (DLM). According to this theory, it is proven that the PE condition of the associated subvector of the radial basis function (RBF) along periodic or quasi-periodic trajectories is satisfied, which guarantees the convergence of the NN approximation error.

Indeed, it is noted that the level of PE, which represents the lower bound of the PE condition, can significantly impact the speed and accuracy of NN in approximating unknown dynamics. In [28], it was demonstrated that both the level and the upper bound of PE influence the performance of the controller, indicating that a higher level of PE results in faster convergence and improved accuracy of the controller. For the devel-

oped AHGO methods [13, 29], the impact of the PE condition on observer performance has not been analyzed, leaving it unclear how the level of PE affects convergence speed and accuracy. Furthermore, how the PE level of the regressor subvector of the observer NN $S_\zeta(Z)$ influences the convergence speed and accuracy of the controller remains an unresolved issue.

The innovations of this paper lie in the following aspects:

1. In this paper, the AHGO is developed, in which NNs are employed to compensate for unknown dynamics, resulting in enhanced estimation accuracy compared to traditional high-gain observers. Consequently, a relatively lower observer gain can be selected, which reduces the impact of measurement noise.
2. In contrast to the presented AHGO [13, 29], which lacks a detailed explanation of how the level of PE affects observer convergence speed and accuracy, our study offers a comprehensive analysis of this relationship. Through convergence analysis in adaptive estimation, we rigorously investigate the influence of the PE level on the convergence performance of the AHGO. It is noted that a higher PE level also helps mitigate the effects of measurement noise.
3. In [30], the relationship between observer gain and controller performance is analyzed. However, in the presence of measurement noise, there exists a trade-off between speed and accuracy: as the observer gain increases, control speed improves, but accuracy declines. In this paper, it is noted that the controller's properties (i.e., control speed and accuracy) are not only influenced by the observer and control gains, but also by the level of PE of the observer NN. Through this connection, the desired control performance can be obtained by setting the appropriate level of PE.

The structure of this paper is as follows. Section 2 presents the problem formulation. Section 3 shows the design of AHGO, and the convergence analysis of the states and NN weights under the effect of PE level. In Sect. 4, the adaptive NN controller is derived, and its performance is strictly analyzed. In Sect. 5, simulation results are presented to exhibit the effectiveness of the developed method. Section 6 presents the conclusion of this article.

2 Problem formulation

2.1 Problem formulation

Consider a class of nonlinear systems as

$$\begin{cases} \dot{x} = A_o x + B_o (\phi(x) + g(x)u), \\ y = C_o x + d(t), \end{cases} \quad (1)$$

where

$$A_o = \begin{bmatrix} 0 & 1 & \cdots & 0 \\ \vdots & \vdots & \ddots & \vdots \\ 0 & 0 & \cdots & 1 \\ 0 & 0 & \cdots & 0 \end{bmatrix}, \quad B_o = \begin{bmatrix} 0 \\ 0 \\ \vdots \\ 1 \end{bmatrix}, \quad C_o = [1 \ 0 \ \cdots \ 0],$$

$x \in \mathcal{R}^n$ denotes the unavailable state vector, $y \in \mathcal{R}$ represents the output vector, and $u \in \mathcal{R}^m$ is the control input vector. The mappings $\phi(x) : \mathcal{R}^n \mapsto \mathcal{R}$ and $g(x) : \mathcal{R}^n \mapsto \mathcal{R}$ are unknown nonlinear functions, and $d(t) \in \mathcal{R}$ represents the measurement noise. To reduce complexity, we omit the time term (t) and use d instead of $d(t)$.

Consider the following assumptions:

Assumption 1 The system states trajectory is a periodic or quasi-periodic motion, i.e., $\forall t \geq t_0, (x, u) \in \mathcal{C} \subset \mathcal{R}^{n \times m}$, \mathcal{C} denotes a compact set.

Assumption 2 Let $\gamma(x, u) \triangleq \phi(x) + g(x)u$, and $\gamma(x, u)$ is Lipschitz continuous, i.e.,

$$|\gamma(\hat{x}, u) - \gamma(x, u)| \leq k_\gamma |\hat{x} - x|, \quad (2)$$

where k_γ is a Lipschitz constant and \hat{x} denotes the estimation of x .

Assumption 3 The nonlinear function $\gamma_u(x, u) = \frac{\partial \gamma(x, u)}{\partial u} \neq 0$, for all $(x, u) \in \mathcal{R}^n \times \mathcal{R}$ and there exist smooth functions $\gamma_1(x)$ and constant $\gamma_0 > 0$ such that $0 < \gamma_0 \leq \gamma_u(x, u) < \gamma_1(x)$.

Remark 1 Assumption 2 is a standard assumption to ensure that the solution $x(t)$ of the system (1) is unique for any finite initial condition. Many types of nonlinearities in practical systems can be assumed to be Lipschitz; for instance, x^2 is a local Lipschitz nonlinearity, and the sinusoidal functions commonly encountered in robotic problems are all globally Lipschitz [31]. In this

paper, u is designed to allow y to track the recurrent trajectory y_r , which implies that y is also a recurrent trajectory. Thus, $\gamma(x, u)$ is globally Lipschitz, and the curve of $\gamma(x, u)$ under the designed input u is illustrated in Fig. 3(a), verifying that Assumption 2 is satisfied.

2.2 Localized RBF NNs and partial PE condition

The RBF NNs can be utilized to approximate the unknown function $\gamma(Z) : \Omega_z \rightarrow \mathcal{R}$ with $\Omega_z \subset \mathcal{R}^N$.

$$\gamma(Z) = S^T(Z)W^* + \epsilon, \quad Z \in \Omega_z \quad (3)$$

where $W^* \in \mathcal{R}^p$ is the ideal weight vector, $S(Z) \in \mathcal{R}^p$ denotes the RBF neurons vector, $Z = [\hat{x}, u] \subset \Omega_z \in \mathcal{R}^N$ denotes the NN input vector, p is the number of NN nodes, and the reconstruct error $\epsilon > 0$.

By utilizing the spatially localized approximation ability of RBF NNs, along the system trajectory, the output of $S^T(\hat{x}, u)\hat{W}$ is primarily impacted by the sub-network $S_\zeta^T(\hat{x}, u)\hat{W}_\zeta$ (see [27] for more details), one has

$$\gamma(Z) = S_\zeta^T(Z)W_\zeta^* + \epsilon_\zeta, \quad (4)$$

where $W_\zeta^* \in \mathcal{R}^{p_\zeta}$ and $S_\zeta(Z) \in \mathcal{R}^{p_\zeta}$ denote the sub-vectors of W^* and $S(Z)$, respectively, $p_\zeta \leq p$, and the reconstruct error $\epsilon_\zeta > 0$.

Remark 2 The sub-network is a localized RBF NN designed to approximate the unknown system dynamic. One of the most prominent features of RBF NN is its localized approximation capability. Specifically, when the input signal enters the RBF NN, only a subset of neurons close to the input trajectory is activated simultaneously. As a result, the output of the RBF NN is influenced solely by the activated neurons and their respective weights. This localized approximation capability indicates that the RBF NN can approximate any continuous function $f(Z)$ with a finite number of neurons [32]. Specifically, the activated neurons and their respective weights constitute the sub-network.

As is widely known, strict PE condition must be satisfied to ensure the convergence of NN weights [26]. Recently, a DLM was presented by Wang et al. [27]. This theory presents that the associated subvector of the RBF along a periodic or quasi-periodic trajectory

satisfies the PE condition, which is called partial PE. For simplicity, we still refer to it as the PE condition.

Lemma 1 *For a periodic trajectory Z in a compact set Ω_z , there exist constants $\delta, \lambda_1, \lambda_2 > 0$ that $S_\zeta(Z)$ is PE [27]*

$$\lambda_1 I \leq \int_t^{t+\delta} S_\zeta(Z) S_\zeta^T(Z) d\tau \leq \lambda_2 I, \forall t \geq t_0 \quad (5)$$

where I denotes the identity matrix, λ_1 and λ_2 can be defined as the PE level and the upper bound of PE, respectively.

Remark 3 In this paper, to address the tracking problem, u must be designed to track the periodic reference signal y_r . In this case, u can ensure Assumption 1 is satisfied. Additionally, bounded disturbances will cause the state to exhibit quasi-periodic behavior. In [27], it is demonstrated that not only the periodic trajectories, but also quasi-periodic trajectories can let $S_\zeta(Z)$ satisfy the PE condition.

3 Adaptive high gain observer

In this part, the AHGO is constructed to estimate the system states x and unknown system dynamic $\gamma(x, u)$ simultaneously. Thus, one has

$$\begin{cases} \dot{\hat{x}} = A_o \hat{x} + \rho \Delta \kappa_o (y - C_o \hat{x}) \\ + \Delta \Upsilon \Omega^{-1} \dot{\tilde{W}} + B_o S^T(\hat{x}, u) \hat{W}, \\ \dot{\tilde{W}} = \Omega \Gamma (C_o \Upsilon)^T (y - C_o \hat{x}), \end{cases} \quad (6)$$

where \hat{x} is the estimated state vector, $\Delta = \text{diag}\{1, \rho, \rho^2, \dots, \rho^{n-1}\} \in \mathcal{R}^{n \times n}$, $\Gamma \in \mathcal{R}^{p \times p}$ is a symmetric positive definite constant matrix, $\Omega = \text{diag}\{\rho^{n-1}, \rho^{n-1}, \dots, \rho^{n-1}\} \in \mathcal{R}^{p \times p}$, the constant high gain $\rho > 0$, the constant observer gain is derived by $\kappa_o = (2Q)^{-1} C_o^T$, $S^T(\hat{x}, u) \hat{W}$ is the RBF NN that is constructed to approximate the unknown function $\gamma(x, u)$. The constant matrix Q satisfies the following equation [14]:

$$A_o^T Q + Q A_o + Q = C_o^T C_o. \quad (7)$$

$\Upsilon \in \mathcal{R}^{n \times p}$ is a time-varying matrix which can be derived by

$$\dot{\Upsilon} = \rho A_1 \Upsilon + B_o S^T(\hat{x}, u), \quad (8)$$

where $A_1 = A_o - \kappa_o C_o$.

By utilizing the spatially localized approximation ability of RBF NNs, the observer (6) is expressed as

$$\begin{cases} \dot{\hat{x}} = A_o \hat{x} + \rho \Delta \kappa_o (y - C_o \hat{x}) + \Delta \Upsilon \Omega^{-1} \dot{\tilde{W}}, \\ + B_o S_\zeta^T(\hat{x}, u) \hat{W}_\zeta, \\ \dot{\tilde{W}}_\zeta = \Omega_\zeta \Gamma_\zeta (C_o \Upsilon_\zeta)^T (y - C_o \hat{x}), \end{cases} \quad (9)$$

where $\Omega_\zeta = \text{diag}\{\rho^{n-1}, \rho^{n-1}, \dots, \rho^{n-1}\} \in \mathcal{R}^{p_\zeta \times p_\zeta}$, $\Gamma_\zeta \in \mathcal{R}^{p_\zeta \times p_\zeta}$, the filter $\Upsilon_\zeta \in \mathcal{R}^{n \times p_\zeta}$ is designed as

$$\begin{aligned} \dot{\Upsilon}_\zeta &= \rho A_1 \Upsilon_\zeta + B_o S_\zeta^T(\hat{x}, u), \\ r &= C_o \Upsilon_\zeta, \end{aligned} \quad (10)$$

where r is the output of the filter, which is time-varying.

Since A_1 is Hurwitz and $S_\zeta^T(\hat{x}, u)$ is bounded, it can be easily inferred that Υ_ζ is also bounded. The proof is straightforward, so it is omitted here. It is a useful corollary that will be utilized later.

Define the estimation errors \tilde{x} and \tilde{W}_ζ as

$$\begin{cases} \tilde{x} = \hat{x} - x, \\ \tilde{W}_\zeta = \hat{W}_\zeta - W_\zeta^*. \end{cases} \quad (11)$$

Recalling (1) and (9), the error dynamics can be derived as

$$\begin{cases} \dot{\tilde{x}} = (A_o - \rho \Delta \kappa_o C_o) \tilde{x} + \Delta \Upsilon \Omega_\zeta^{-1} \dot{\tilde{W}}_\zeta \\ + B_o (S_\zeta^T(\hat{x}, u) \tilde{W}_\zeta + \tilde{\gamma} - \epsilon_\zeta) + \rho \Delta \kappa_o d, \\ \dot{\tilde{W}}_\zeta = \Omega_\zeta \Gamma_\zeta (C_o \Upsilon_\zeta)^T (C_o \tilde{x} + d), \end{cases} \quad (12)$$

where $\tilde{\gamma} = \gamma(\hat{x}, u) - \gamma(x, u)$.

Problem 1: The first objective is to provide a detailed quantitative analysis of the PE level on the performance of the AHGO. Specifically, we will derive the solution of system (12) in the following desired format

$$\|\chi(t)\| \leq \bar{m} e^{-\lambda(t-t_0)} \|\chi(t_0)\| + \frac{\bar{m}}{\lambda} \rho^{n-1} \bar{\epsilon}', \quad (13)$$

where $\chi(t) = [\tilde{x}(t) \ \tilde{W}_\zeta(t)]^T$, λ denotes the convergence speed, and $\frac{\bar{m}}{\lambda} \rho^{n-1} \bar{\epsilon}'$ represents steady estimation error (12). In this stage, we will examine how the PE level affects the performance of AHGO, paying particular attention to the accuracy and speed of learning,

which will be evaluated in terms of λ and \bar{m} . To summarize, we aim to establish the connection between the PE level of $S_\zeta^T(\hat{x}, u)$ with λ and \bar{m} .

4 Main results

4.1 The influence of PE level on the performance of AHGO

Theorem 1 Considering the error system (12), under Assumptions 1 and 2, and Lemma 1, the explicit solution of system (12) can be derived by

$$\|\chi(t)\| \leq \bar{m} e^{-\lambda(t-t_0)} \|\chi(t_0)\| + \frac{\bar{m}}{\lambda} \rho^{n-1} \bar{\epsilon}', \quad (14)$$

with

$$\begin{aligned} \lambda &= \frac{1}{2\delta} \ln \\ &\left(\frac{1}{1 - \mu_3 \lambda_1 b_3 / (2\rho \lambda_{\max}(QP)(1 + (n+m)\lambda_\zeta \alpha_2 \sqrt{2v})^2)} \right), \end{aligned} \quad (15)$$

$$\bar{\epsilon}' = \max \{ \|\rho \kappa_o\|, \|\Gamma_\zeta r^T\| \} \cdot \bar{d} + \|\epsilon'\|, \quad (16)$$

where \bar{d} denotes the upper bound of $\|d(t)\|$, and $\bar{m} \propto 1/\lambda_1$ and $\bar{m} \propto \lambda_2$ is bounded. It is noted that by selecting appropriate parameters, such as the observer gain ρ , λ_1 or λ_2 , the term in $\ln()$ > 0 can be ensured.

Proof In this Theorem, we aim to investigate the convergence properties of system (12). To achieve this, we utilize the UCO and “output injection” methods, which are commonly employed in the stability analysis of adaptive systems [33], the explicit solution (14) of the error system (12) can be acquired under the PE condition of $S_\zeta^T(\hat{x}, u)$. There are four steps in the proof, we will incorporate certain conclusions from our previous papers as part of the proof. These conclusions will be directly utilized here without providing specific proof processes [13].

Step 1: In this Step, we aim to prove the filter signal r in (10) is PE. The proof in this Step is overly intricate. We will reference the earlier conclusion, and for a thorough derivation, please consult document [13].

The special structure of C_o determines that κ_o must be a column vector, i.e., for $(2Q)^{-1} = \begin{bmatrix} Q_{11} & \cdots & Q_{1n} \\ \vdots & \ddots & \vdots \\ Q_{n1} & \cdots & Q_{nn} \end{bmatrix}$,

we have $\kappa_o = (2Q)^{-1} C_o^T = \begin{bmatrix} Q_{11} & \cdots & Q_{1n} \\ \vdots & \ddots & \vdots \\ Q_{n1} & \cdots & Q_{nn} \end{bmatrix} \times$

$$\begin{bmatrix} 1 \\ 0 \\ \vdots \\ 0 \end{bmatrix} = \begin{bmatrix} Q_{11} \\ \vdots \\ Q_{n1} \end{bmatrix} \triangleq [k_1, k_2, \dots, k_n]^T. \text{ Then, we have}$$

$$\begin{aligned} A_1 &= A_o - \kappa_o C_o = \begin{bmatrix} 0 & 1 & \cdots & 0 \\ \vdots & \vdots & \ddots & \vdots \\ 0 & 0 & \cdots & 1 \\ 0 & 0 & \cdots & 0 \end{bmatrix} - \begin{bmatrix} k_1 \\ k_2 \\ \vdots \\ k_n \end{bmatrix} \begin{bmatrix} 1 & 0 & \cdots & 0 \end{bmatrix} \\ &= \begin{bmatrix} -k_1 & 1 & \cdots & 0 \\ \vdots & \vdots & \ddots & \vdots \\ -k_{n-1} & 0 & \cdots & 1 \\ -k_n & 0 & \cdots & 0 \end{bmatrix}. \end{aligned} \quad (17)$$

Define the transfer function from $S_\zeta^T(\hat{x}, u)$ to r as $H(s)$. Since $H(s)$ are minimum phase and strictly proper stable, there are some positive constants b_1 and b_2 [13], then, we have

$$|h(t)| \leq b_1 e^{-b_2 t}, \quad (18)$$

where $h(t)$ denotes the impulse response of $H(s)$.

Recalling the filter (10), under Assumption 2 and Lemma 2.6.7 in [33], the signal $r(t)$ is PE. Therefore, we can get

$$\alpha_1 I \leq \int_{t_0}^{t_0+v} r^2 d\tau \leq \alpha_2 I, \quad (19)$$

where α_1 and α_2 define the level and the upper bound of PE signal r , respectively. According to the Lemma 4.8.3 in [34], it can be inferred that $\alpha_1 = \lambda_1 b_3$ with $b_3 > 0$ which is related to $\|H(s)\|_\infty^2$, $\alpha_2 = \lambda_2 b_4$ with $b_4 > 0$ which is related to $\rho, h(t)$ and $\sup_\tau \|S_\zeta^T(\hat{x}, u)\|$. Noted that α_1 is positive related to λ_1 , and α_2 is positive related to λ_2 . Constants α_1 and α_2 serve as a bridge to establish the relationship between λ_1 , and λ_2 with λ .

Step 2: In this Step, we provide a system transformation of (12). The error system (23) consists of a nominal

part and a disturbance part. The nominal part primarily influences the convergence rate (i.e., the learning speed of the algorithm), while the disturbance part mainly affects the convergence bound (i.e., the learning accuracy of the algorithm). By solving for the state transition matrix of (24), we can obtain the state transition matrix of (23). To achieve this, the UCO of system (24) needs to be given.

Let $\tilde{z} = \Delta^{-1}\tilde{x}$ and $\vartheta = \Omega_\zeta^{-1}\tilde{W}_\zeta$. According to the special forms of A_o , B_o and C_o , it is no hard to obtain that $C_o\Delta = C_o$, $A_o\Delta = \rho\Delta A_o$ and $\Delta^{-1}B_o = B_o\rho^{-n+1}$. Then, the system (12) becomes

$$\dot{\tilde{z}} = \rho A_1\tilde{z} + \Upsilon_\zeta\dot{\vartheta} + B_oS_\zeta^T(\hat{x}, u)\vartheta + \epsilon' + \xi + \rho\kappa_o d, \quad (20)$$

where $\epsilon' = -\Delta^{-1}B_o\epsilon_\zeta$ and $\xi = -\Delta^{-1}B_o\tilde{\gamma}$.

Let $\eta = \tilde{z} - \Upsilon_\zeta\vartheta$, it can be inferred that

$$\begin{aligned} \dot{\eta} &= \rho A_1(\eta + \Upsilon_\zeta\vartheta) + B_oS_\zeta^T(\hat{x}, u)\vartheta \\ &\quad - \dot{\Upsilon}_\zeta\vartheta + \epsilon' + \xi + \rho\kappa_o d \\ &= \rho A_1\eta + \epsilon' + \xi + \rho\kappa_o d. \end{aligned} \quad (21)$$

Since $\vartheta = \Omega_\zeta^{-1}\tilde{W}_\zeta$, it follows that

$$\begin{aligned} \dot{\vartheta} &= \Omega_\zeta^{-1}\Omega_\zeta\Gamma_\zeta\Upsilon_\zeta^T C_o^T(y - \hat{y}) \\ &= -\Gamma_\zeta\Upsilon_\zeta^T C_o^T(C_o\tilde{x} + d) \\ &= -\Gamma_\zeta\Upsilon_\zeta^T C_o^T(C_o\Delta\tilde{z} + d) \\ &= -\Gamma_\zeta\Upsilon_\zeta^T C_o^T(C_o(\eta + \Upsilon_\zeta\vartheta) + d). \end{aligned} \quad (22)$$

Based on (21) and (22), one has

$$\begin{bmatrix} \dot{\eta} \\ \dot{\vartheta} \end{bmatrix} = \begin{bmatrix} \rho A_1 & 0 \\ -\Gamma_\zeta r^T C_o & -\Gamma_\zeta r^T r \end{bmatrix} \begin{bmatrix} \eta \\ \vartheta \end{bmatrix} + \begin{bmatrix} \rho\kappa_o \\ -\Gamma_\zeta r^T \end{bmatrix} d + \begin{bmatrix} \epsilon' + \xi \\ 0 \end{bmatrix}. \quad (23)$$

Based on Lemma 2, we can prove the following nominal system (disturbance-free version of (23)) is UCO

$$\begin{bmatrix} \dot{\eta} \\ \dot{\vartheta} \end{bmatrix} = \begin{bmatrix} \rho A_1 & 0 \\ 0 & 0 \end{bmatrix} \begin{bmatrix} \eta \\ \vartheta \end{bmatrix} + \begin{bmatrix} 0 \\ -\Gamma_\zeta r^T \end{bmatrix} [C_o \ r] \begin{bmatrix} \eta \\ \vartheta \end{bmatrix},$$

$$Y_1 = [C_o \ r] \begin{bmatrix} \eta \\ \vartheta \end{bmatrix}. \quad (24)$$

Lemma 2 (Lemma 2.5.2 in [33]) *For $\delta > 0$, there exists $K_\delta \geq 0$ such that, for all $t_0 \geq 0$*

$$\int_{t_0}^{t_0+\delta} \|K(\tau)\|^2 d\tau \leq K_\delta, \quad (25)$$

Then, the system $[C, A]$ is UCO if and only if the system $[C, A + KC]$ is UCO. Moreover, for positive constants β_1 and β_2 , the observability grammian of the system $[C, A]$ satisfies

$$\beta_2 I \geq N(t_0, t_0 + \sigma) \geq \beta_1 I, \quad (26)$$

then the observability grammian of the system $[C, A + KC]$ satisfies these inequalities with identical σ and

$$\begin{aligned} \beta'_1 &= \beta_1 / (1 + \sqrt{k_\delta \beta_2}), \\ \beta'_2 &= \beta_2 \exp(k_\delta \beta_2). \end{aligned} \quad (27)$$

Let $K(\tau) = \begin{bmatrix} 0 \\ -\Gamma_\zeta r^T \end{bmatrix}$, which represents the output injection term of (24), for $\delta = (m+n)v$, $m > 0$, $v > 0$ and $n > 0$, one has

$$\int_{t_0}^{t_0+\delta} \|K(\tau)\|^2 d\tau \leq \lambda_\zeta^2 \alpha_2 \delta = K_\delta, \quad (28)$$

where λ_ζ denotes the maximum eigenvalue of Γ_ζ .

According to Lemma 2, it can be derived that

$$\begin{aligned} \alpha_3 (\|\eta(t_0)\|^2 + \|\vartheta(t_0)\|^2) &\geq \int_{t_0}^{t_0+\delta} Y_1^2(\tau) d\tau \\ &\geq \alpha_4 (\|\eta(t_0)\|^2 + \|\vartheta(t_0)\|^2), \end{aligned} \quad (29)$$

where $\alpha_3 = 2(n+m)\alpha_2 e^{2(n+m)\alpha_2 K_\delta}$ and $\alpha_4 = \frac{\alpha_1}{\rho(1+(n+m)\lambda_\zeta\alpha_2\sqrt{2v})^2}$. Then, we can derive the UCO of (24), the inequality (29) will be used in Step 3.

Due to space constraints, the detailed derivation of (29) will be omitted. For more details, please refer to Theorem 1 in [28], Lemma 4.8.1 in [34], or Lemma 3 in [13].

Step 3: In this Step, we conduct stability analysis of the transformed states to lay the groundwork for Step 4.

Consider the linear time varying system as

$$\dot{\omega}(t) = -\Gamma_\zeta r^T(t)r(t)\omega(t),$$

$$y_\omega = r\omega, \quad (30)$$

where ω is the system state, and y_ω is the output of the linear time varying system.

Since r is PE, it can be easily seen that the UCO system (30) is exponentially stable. Based on the Theorem 1.5.6 in [33], there is a symmetric positive definite time-varying matrix $P(t) \in \mathcal{R}^{n \times n}$, we have

$$\dot{P}(t) = (\Gamma_\zeta r^T r)^T P(t) + P(t)(\Gamma_\zeta r^T r) - I, \quad (31)$$

where $P(t)$ is known to have positive lower and upper bounds [15].

To obtain the explicit solution of disturbance-free system (24), consider the Lyapunov function candidate as

$$V = \eta^T Q \eta + \vartheta^T P(t) \vartheta. \quad (32)$$

Recalling the special forms of (7) and κ_o , and taking the derivative of V along with (24), we have

$$\begin{aligned} \dot{V} = & -\rho \eta^T Q \eta - 2\vartheta^T P \Gamma_\zeta r^T C_o (\eta + \Upsilon_\zeta \vartheta) \\ & + 2\vartheta^T P \Gamma_\zeta r^T C_o \Upsilon_\zeta \vartheta - \vartheta^T \vartheta. \end{aligned} \quad (33)$$

Since Υ_ζ is bounded, let μ_1 denotes the upper bound of $\|P \Gamma_\zeta r\|$. According to Young's inequality, we obtain

$$2\vartheta^T P \Gamma_\zeta r^T C_o \eta \leq \frac{2\mu_1^2}{\rho \mu_q} \|\vartheta\|^2 + \frac{1}{2} \rho \mu_q \|\eta\|^2, \quad (34)$$

where μ_q denotes the minimum eigenvalue of Q .

Substituting (34) into (33), one has

$$\begin{aligned} \dot{V} \leq & -\rho \mu_q \|\eta\|^2 + \frac{1}{2} \rho \mu_q \|\eta\|^2 + \frac{2\mu_1^2}{\rho \mu_q} \|\vartheta\|^2 - \|\vartheta\|^2. \end{aligned} \quad (35)$$

Choose the suitable gain ρ , such that

$$1 - \frac{2\mu_1^2}{\rho \mu_q} > \frac{1}{2}. \quad (36)$$

Then, we obtain

$$\dot{V} \leq -\frac{1}{2} \rho \mu_q \|\eta\|^2 - \frac{1}{2} \|\vartheta\|^2. \quad (37)$$

Obviously, according to (32), we have

$$V \leq \lambda_{\max(QP)} (\|\eta\|^2 + \|\vartheta\|^2), \quad (38)$$

where $\lambda_{\max(QP)} = \max\{\lambda_{\max(P)}, \lambda_{\max(Q)}\}$.

By integrating both sides of (37) and utilizing the results from Step 2, we obtain

$$\begin{aligned} \int_t^{t+\delta} \dot{V} d\tau & \leq - \left(\int_t^{t+\delta} \frac{1}{2} \rho \mu_q \|\eta\|^2 + \frac{1}{2} \|\vartheta\|^2 d\tau \right) \\ & \leq -\mu_2 \left(\int_t^{t+\delta} \|\eta\|^2 + \|\vartheta\|^2 d\tau \right) \\ & \leq -\mu_2 \left(\int_t^{t+\delta} \|C_o \eta\|^2 + \frac{\|r\|^2}{\bar{h}^2} \|\vartheta\|^2 d\tau \right) \\ & \leq -\mu_3 \left(\int_t^{t+\delta} \|C_o \eta\|^2 + \|r \vartheta\|^2 d\tau \right) \\ & \leq -\frac{\mu_3}{2} \int_t^{t+\delta} \|Y_1\|^2 d\tau \\ & \leq -\frac{\mu_3}{2} \alpha_4 (\|\eta(t)\|^2 + \|\vartheta(t)\|^2), \end{aligned} \quad (39)$$

where $\mu_2 = \min\{\frac{1}{2} \rho \mu_q, \frac{1}{2}\}$, $\mu_3 = \mu_2 / \bar{h}^2$, $\bar{h} = \max\{\bar{r}, 1\}$, and $\bar{r} = \sup_{t > t_0} \{\|r\|\}$.

Step 4: With the aid of Lemma 1.5.2 in [33] or Theorem 1 in [28], we can obtain an explicit solution of disturbance-free system (24). Then, we can get the state transition matrix $\Phi(t, t_0)$ of the disturbance system (23). Finally, the explicit solution of the error system (12) can be obtained.

By using the Lemma 1.5.1 in [33] (the detail derivation can be found in the Lemma 2 of [35]), the convergence speed α_v of $V(t)$ is derived. Firstly, in terms of (39), one has

$$\begin{aligned} V(t) - V(t + \delta) & \geq \frac{\mu_3}{2} \alpha_4 (\|\eta(t)\|^2 + \|\vartheta(t)\|^2) \\ & \geq \frac{\mu_3}{2 \lambda_{\max(QP)}} \alpha_4 V(t) = \mu_4 V(t), \end{aligned} \quad (40)$$

where $\mu_4 = \frac{\mu_3}{2 \lambda_{\max(QP)}} \alpha_4$.

Then, we can get

$$(1 - \mu_4) V(t) \geq V(t + \delta). \quad (41)$$

Therefore, $V(t)$ decays exponentially

$$(1 - \mu_4)^{k_v} V(t_0) \geq V(t_0 + k_v \delta), \quad (42)$$

where $k_v > 0$.

In order to calculate the decay time constant, we define

$$e^{-a_v k_v \delta} V(t_0) \geq V(t_0 + k_v \delta), \quad (43)$$

$$\text{where } e^{-a_v k_v \delta} = (1 - \mu_4)^{k_v}.$$

Then, the decay constant can be obtained as

$$a_v = -\frac{1}{\delta} \ln(1 - \mu_4), \quad (44)$$

and let $t - t_0 = k_v \delta$, one has

$$V(t) \leq e^{-a_v(t-t_0)} V(t_0). \quad (45)$$

Recall the definition of V (32), we can get

$$\|\chi'(t)\| \leq \bar{m} e^{-\lambda(t-t_0)} \|\chi'(t_0)\|, \quad (46)$$

where $\chi'(t) = [\eta(t) \ \vartheta(t)]^T$, since $P^{-1}(t)$ is bounded, \bar{m} is the maximum eigenvalue of $\begin{bmatrix} 1 & 0 \\ 0 & P^{-1}(t)P(0) \end{bmatrix}^{1/2}$, and

$$\lambda = \frac{1}{2\delta} \ln \left(\frac{1}{1 - \mu_3 \lambda_1 b_3 / (2\rho \lambda_{\max}(QP)(1 + (n+m)\lambda_\zeta \alpha_2 \sqrt{2v})^2)} \right).$$

The following Lemma is provided to give the lower bound of $P(t)$.

Lemma 3 Consider system (30), if r is PE, which means that the condition (19) holds, then one has

$$P(t) \geq \frac{\alpha_5}{\bar{r}^2} \alpha_1, \quad (47)$$

$$\text{where } \alpha_5 = \alpha_1 / (1 + \lambda_\zeta \alpha_2)^2.$$

Proof Recalling system (30), since r is PE, similar to Theorem 2.5.1 in [33], it can be seen that the pair $[r, 0]$ is UCO. Therefore, with the output injection $K_{r\delta} = -\Gamma_\zeta r^T(t)$, the pair $[r, -\Gamma_\zeta r^T(t)r(t)]$ is also UCO. Note that

$$\begin{aligned} K_{r\delta} &= \int_t^{t+\delta} \|K_{r\delta}(\tau)\|^2 d\tau \\ &= \int_t^{t+\delta} \|\Gamma_\zeta r^T(t)\|^2 d\tau \leq \lambda_\zeta^2 \alpha_2 \delta. \end{aligned} \quad (48)$$

Based on Lemma 2, we have

$$\int_t^{t+\delta} (r(\tau) \omega(\tau))^2 d\tau \geq \alpha_5 \omega(t). \quad (49)$$

Based on (49), we have

$$\begin{aligned} \int_t^{t+\delta} \omega^T(\tau) \omega(\tau) d\tau &\geq \int_t^{t+\delta} \frac{1}{\bar{r}^2} (r(\tau) \omega(\tau))^2 d\tau \\ &\geq \frac{\alpha_5}{\bar{r}^2} \|\omega(t)\|^2. \end{aligned} \quad (50)$$

Since $\Phi_w(\tau, t) \omega(t) = \omega(\tau)$, we have

$$\begin{aligned} P(t) &= \int_t^\infty \Phi_w^T(\tau, t) \Phi_w(\tau, t) d\tau \\ &\geq \int_t^{t+\delta} \Phi_w^T(\tau, t) \Phi_w(\tau, t) d\tau \geq \frac{\alpha_5}{\bar{r}^2}. \end{aligned} \quad (51)$$

Then, we can get $P^{-1}(t) \leq \bar{r}^2 / \alpha_5$, which means that $\bar{m} = \max \left\{ \left(P(0) \bar{r}^2 / \alpha_5 \right)^{1/2}, 1 \right\}$.

From (46), the system (23) state transition matrix $\Phi(t, t_0)$ can be expressed as

$$\|\Phi(t, t_0)\| \leq \bar{m} e^{-\lambda(t-t_0)}. \quad (52)$$

The explicit solution $\chi'(t)$ of (23) can be derived by

$$\chi'(t) \leq \Phi(t, t_0) \chi'(t_0) + \int_{t_0}^t \Phi(t, \tau) \bar{\epsilon}' d\tau, \quad (53)$$

$$\text{where } \bar{\epsilon}' = \max \{ \|\rho \kappa_o\|, \|\Gamma_\zeta r^T\| \} \cdot \bar{d} + \|\epsilon'\|.$$

Therefore, by using (52), yields

$$\begin{aligned} \|\chi'(t)\| &\leq \bar{m} e^{-\lambda(t-t_0)} \|\chi'(t_0)\| + \bar{m} \bar{\epsilon}' \int_{t_0}^t e^{-\lambda(t-\tau)} d\tau \\ &\leq \bar{m} e^{-\lambda(t-t_0)} \|\chi'(t_0)\| + \frac{\bar{m}}{\lambda} \bar{\epsilon}'. \end{aligned} \quad (54)$$

Recalling that $\eta = \tilde{z} - \Upsilon_\zeta \vartheta$, $\vartheta = \Omega_\zeta^{-1} \tilde{W}_\zeta$ and $\tilde{z} = \Delta^{-1} \tilde{x}$, we have

$$\chi(t) = \begin{bmatrix} \Delta & \Delta \Upsilon_\zeta \\ 0 & \Omega_\zeta \end{bmatrix} \chi'(t) \leq \rho^{n-1} \Gamma' \chi'(t), \quad (55)$$

$$\text{where } \Gamma' = \begin{bmatrix} I & \Upsilon_\zeta \\ 0 & I \end{bmatrix}.$$

Then, we can get

$$\|\chi(t)\| \leq \bar{m}e^{-\lambda(t-t_0)}\|\chi(t_0)\| + \frac{\bar{m}}{\lambda}\rho^{n-1}\bar{\epsilon}'. \quad (56)$$

This ends the proof. \square

From (56), the relationship between learning speed and accuracy with parameters λ and \bar{m} is revealed. The larger values of λ and $1/\bar{m}$ lead to faster learning speed and higher estimation accuracy, while the lower values of λ and $1/\bar{m}$ result in slower learning speed and lower estimation accuracy. It can be directly seen that \bar{m} is positively correlated with α_2 and negatively correlated with α_1 , which means that \bar{m} is positively correlated with λ_2 and negatively correlated with λ_1 . In the next Corollary, we will investigate the influence of PE condition on parameter λ , aiming to establish the relationship between PE condition and learning speed as well as accuracy.

Corollary 1 Considering the error system (12), and the RBF NN (4), under Assumptions 1 and 2, the influence of PE condition on parameter λ is revealed. According to the expression of λ , it is demonstrated that the learning speed and accuracy are proportional to the level of PE λ_1 and inversely proportional to the upper bound of PE λ_2 .

Proof Recalling the expression of λ , we have

$$\begin{aligned} \lambda &= \frac{1}{2\delta} \ln \left(\frac{1}{1 - \mu_3 \lambda_1 b_3 / (2\rho \lambda_{\max(QP)} (1 + (n+m)\lambda_\zeta \alpha_2 \sqrt{2v})^2)} \right) \\ &\leq \frac{1}{2\delta} \ln \left(\frac{1}{1 - \mu_3 \lambda_1 b_3 / (2\rho \lambda_{\max(QP)} ((n+m)\lambda_\zeta \alpha_2 \sqrt{2v})^2)} \right) \\ &= \frac{1}{2\delta} \ln \left(\frac{1}{1 - \mu_5 \lambda_1 / \lambda_2^2} \right), \end{aligned} \quad (57)$$

where $\mu_5 = \mu_3 b_3 / (2\rho \lambda_{\max(QP)} (2(n+m)b_4^2 \lambda_\zeta^2 \delta))$.

It is important to note that in [28], the impact of the PE level and the upper bound on control speed was discussed separately. However, it is essential to consider the premise that the PE level is always smaller than the upper bound. Therefore, when discussing their impact on control speed and accuracy, it is necessary to consider the PE level and the upper bound simultaneously, avoiding any situation where the PE level exceeds the upper bound.

In light of (57), calculating the partial derivative of λ with respect to λ_1 , it can be easily obtained that

$$\frac{\partial \lambda}{\partial \lambda_1} \leq \frac{1}{2\delta} \left(\frac{\mu_5}{\lambda_2^2 - \mu_5 \lambda_1} \right). \quad (58)$$

Since $1 - \mu_5 \lambda_1 / \lambda_2^2 > 0$, then we can conclude that $\frac{\partial \lambda}{\partial \lambda_1} > 0$ at all times. It can be concluded that the learning speed and accuracy are proportional to the level of PE.

The influence of the upper bound of PE λ_2 on λ can be readily derived in a similar manner as above, therefore, it will be omitted here. \square

The above results have demonstrated that the learning speed and accuracy are proportional to the level of PE λ_1 and inversely proportional to the upper bound of PE λ_2 .

4.2 The influence of PE level on the performance of the output-feedback controller

In this part, the relationship between the PE level of the regressor subvector of observer NN with the control speed and accuracy of the controller are revealed.

Consider the following reference systems

$$\begin{cases} \dot{x}_{ri} = \gamma_{ri}(x_r), & i = 1, 2, \dots, n \\ y_r = C_o x_r, \end{cases} \quad (59)$$

$x_r \in \mathcal{R}^n$ and $y_r \in \mathcal{R}$ denote the state and output vectors of the reference systems, respectively. The mappings $\gamma_{ri}(x_r) : \mathcal{R}^n \mapsto \mathcal{R}$ are smooth known nonlinear functions.

In this part, we aim to design an adaptive controller $u(t)$ for system (1) such that the output y can track the desired trajectory y_r . To achieve this, the RBF NNs are applied to approximate the uncertain system dynamics. The estimated system states, obtained from the AHGO, are utilized as input signals in the adaptive NN controller.

Define the following variables [36]

$$\begin{aligned} Y_r &= [y_r, \dot{y}_r, \dots, y_r^{n-1}]^T, \\ e_r &= Y - Y_r = [y - y_r, \dot{y} - \dot{y}_r, \dots, y^{n-1} - y_r^{n-1}]^T. \end{aligned} \quad (60)$$

Then, the filtered tracking error e_s is expressed as [37]

$$e_s = [\Lambda^T \ 1]e_r, \quad (61)$$

where $\Lambda = [d_1, d_2, \dots, d_{n-1}]^T$ is a coefficient vector and is chosen appropriately, such that the polynomial $s^{n-1} + d_{n-1}s^{n-2} + \dots + d_1$ is Hurwitz.

According to systems (1) and the error vector (60), taking the time derivative of e_s , we have

$$\begin{aligned} \dot{e}_s &= [\Lambda^T \ 1]\dot{e}_r = [0 \ \Lambda^T]e_r + y^n - y_r^n \\ &= \gamma(x, u) - y_r^n + [0 \ \Lambda^T]e_r. \end{aligned} \quad (62)$$

The estimations of e_r and e_s are obtained as follows:

$$\begin{aligned} \hat{e}_r &= \hat{Y} - Y_r = [\hat{y} - y_r, \dot{\hat{y}} - \dot{y}_r, \dots, \hat{y}^{n-1} - y_r^{n-1}]^T, \\ \hat{e}_s &= [\Lambda^T \ 1]\hat{e}_r. \end{aligned} \quad (63)$$

By utilizing the implicit function theorem, it can be seen that there exists a smooth implicit function $\hat{\gamma}(\hat{x}, u^*)$ such that [36]

$$-y_r^n + [0 \ \Lambda^T]\hat{e}_r + \hat{\gamma}(\hat{x}, u^*) = 0, \quad (64)$$

where u^* is the ideal input.

Using the mean value theorem, it follows that:

$$\gamma(x, u) = \gamma(x, u^*) + \gamma_u(u - u^*), \quad (65)$$

where $\gamma_u = \frac{\partial \gamma(x, \bar{u})}{\partial \bar{u}}|_{\bar{u}=u}$ is a smooth unknown function.

Then, we obtain

$$\begin{aligned} \dot{e}_s &= \gamma(x, u) - y_r^n + [0 \ \Lambda^T]e_r \\ &= -y_r^n + [0 \ \Lambda^T]e_r + \gamma(x, u) + \hat{\gamma}(\hat{x}, u^*) - \hat{\gamma}(\hat{x}, u^*) \\ &= \gamma(x, u) + \gamma(x, u^*) - \gamma(x, u^*) \\ &\quad + \gamma(\hat{x}, u^*) - \gamma(\hat{x}, u^*) - \hat{\gamma}(\hat{x}, u^*) \\ &\quad + \hat{\gamma}(\hat{x}, u^*) + [0 \ \Lambda^T]\hat{e}_r - [0 \ \Lambda^T]\tilde{e}_r - y_r^n \\ &= \gamma_u(u - u^*) + k_\gamma \tilde{x} - S_\zeta^T(\hat{x}, u^*)\tilde{W}_\zeta - [0 \ \Lambda^T]\tilde{e}_r, \end{aligned} \quad (66)$$

where $\tilde{e}_r = \hat{e}_r - e_r$. The RBF NN is employed to approximate u^* . Then, we obtain

$$u^* = W_u^{*\top} S_u(Z_u) + \epsilon_u(Z_u), \quad (67)$$

where $Z_u = [\hat{x}, \hat{e}_s]$

The adaptive NN control law can be derived by

$$u = -K\hat{e}_s + \tilde{W}_u^T S_u(Z_u), \quad (68)$$

where $K > 0$ is the controller gain.

The NN weight \tilde{W}_u is updated by

$$\dot{\tilde{W}}_u = \Gamma_u \left(-S_u(Z_u)\hat{e}_s - \sigma_u \tilde{W}_u \right), \quad (69)$$

where $\Gamma_u = \Gamma_u^T > 0$ and $\sigma_u > 0$.

Substituting (67) and (68) into (66), we have

$$\begin{aligned} \dot{e}_s &= \gamma_u \left(-K\hat{e}_s + \tilde{W}_u^T S_u(Z_u) - \epsilon_u(Z_u) \right) \\ &\quad + k_\gamma \tilde{x} - S_\zeta^T(\hat{x}, u^*)\tilde{W}_\zeta - [0 \ \Lambda^T]\tilde{e}_r, \\ \dot{\tilde{W}}_u &= \Gamma_u \left(-S_u(Z_u)\hat{e}_s - \sigma_u (\tilde{W}_u + W_u^*) \right), \end{aligned} \quad (70)$$

where $\tilde{W}_u = \hat{W}_u - \tilde{W}_u^*$.

In the following, the relationship between the PE level of the regressor subvector of observer NN and the speed and accuracy of the controller is revealed.

Theorem 2 Consider the closed-loop system (1) under Assumptions 2 and 3, the controller (68), the AHGO (9), and the adaptive law (69). It can be concluded that the speed and accuracy of the controller are proportional to the level of PE λ_1 and inversely proportional with the upper bound of PE λ_2 .

Proof Consider the Lyapunov candidate function as

$$V_s = \frac{1}{2}\gamma_u^{-1}e_s^2 + \frac{1}{2}\tilde{W}_u^T \Gamma_u^{-1} \tilde{W}_u. \quad (71)$$

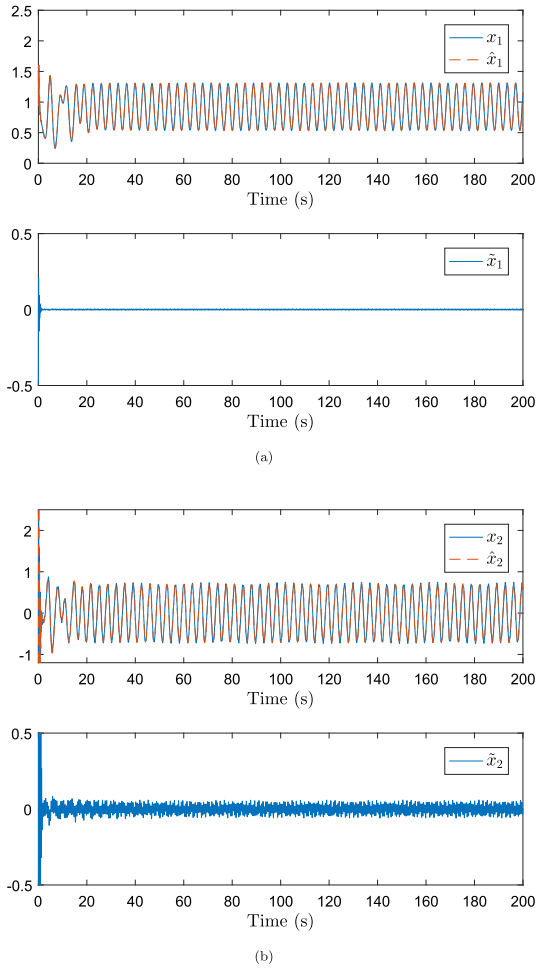
Noting that $\tilde{e}_s = [\Lambda^T \ 1]\tilde{x}$ is convergent, choosing either \hat{e}_s or e_s in the Lyapunov candidate function can indicate the convergence of e_s .

Note that the equalities $\tilde{e}_r = \tilde{x}$ and $\tilde{e}_s = [\Lambda^T \ 1]\tilde{x}$ can be easily induced from (60) and (63) as follows:

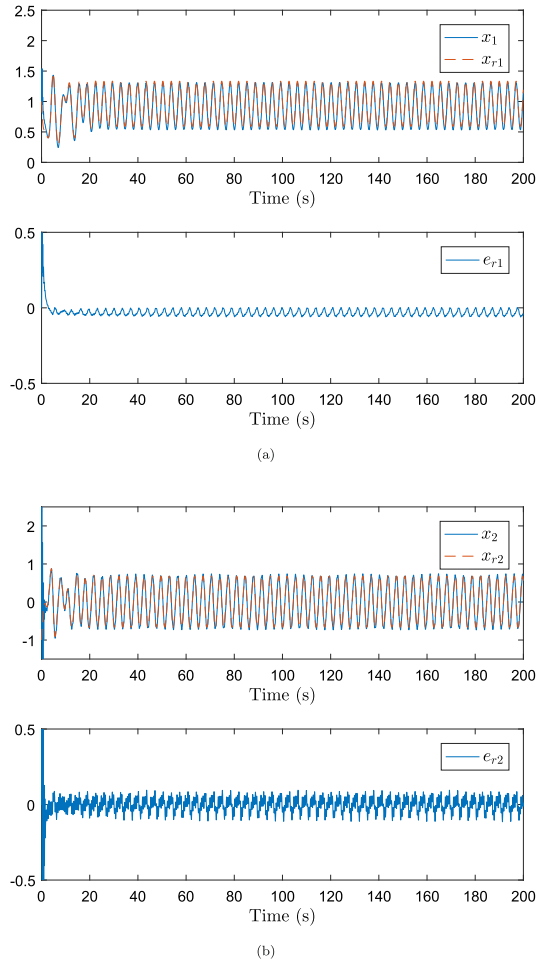
$$\begin{aligned} \tilde{e}_r &= \hat{e}_r - e_r = \hat{Y} - Y = [\hat{y} - y, \dot{\hat{y}} - \dot{y}, \dots, \hat{y}^{n-1} - y^{n-1}]^T = \tilde{x}, \\ \tilde{e}_s &= [\Lambda^T \ 1]\tilde{e}_r = [\Lambda^T \ 1]\tilde{x}. \end{aligned} \quad (72)$$

Taking the time derivative of V_s along system (70), one has

$$\dot{V}_s = \gamma_u^{-1}e_s \dot{e}_s + \tilde{W}_u^T \Gamma_u^{-1} \dot{\tilde{W}}_u$$

**Fig. 1** Convergence of \hat{x}_1 and \hat{x}_2

$$\begin{aligned}
&= -\gamma_u^{-1} e_s [0 \ \Lambda^T] \tilde{x} + e_s (-K(e_s + \tilde{e}_s) \\
&\quad + \tilde{W}_u^T S_u(Z_u) - \epsilon_u(Z_u)) \\
&\quad + \gamma_u^{-1} e_s (k_\gamma \tilde{x} - S_\zeta^T(\hat{x}, u^*) \tilde{W}_\zeta) \\
&\quad + \tilde{W}_u^T (-S_u(Z_u)(e_s + \tilde{e}_s) - \sigma_u(\tilde{W}_u + W_u^*)) \\
&= -\gamma_u^{-1} e_s [0 \ \Lambda^T] \tilde{x} + e_s (-K[\Lambda^T \ 1] \tilde{x} \\
&\quad + \tilde{W}_u^T S_u(Z_u) - \epsilon_u(Z_u)) \\
&\quad + \gamma_u^{-1} e_s (k_\gamma \tilde{x} - S_\zeta^T(\hat{x}, u^*) \tilde{W}_\zeta) \\
&\quad + \tilde{W}_u^T (-S_u(Z_u)(e_s + [\Lambda^T \ 1] \tilde{x}) - \sigma_u W_u^*) \\
&\quad - K e_s^2 - \sigma_u \tilde{W}_u^T \tilde{W}_u. \tag{73}
\end{aligned}$$

**Fig. 2** Desired and actual states x_{r1} , x_{r2} , x_1 and x_2

Let $c_{\Lambda 1} = \|[\Lambda^T \ 1]\|$, $c_{\Lambda 2} = \|[0 \ \Lambda^T]\|$. Since $S_u(Z_u)$ is bounded, let c_1 denotes the upper bound of $\|S_u(Z_u)\|$ and $k_{\Lambda 1} = \|K[\Lambda^T \ 1]\|$, we obtain

$$\begin{aligned}
\dot{V}_s &\leq -\|e_s\|(\theta_1 \|e_s\| - \gamma_0^{-1} c_{\Lambda 2} \|\tilde{x}\| - \\
&\quad k_{\Lambda 1} \|\tilde{x}\| - \|\epsilon_u(Z_u)\| - \gamma_0^{-1} k_\gamma \|\tilde{x}\| \\
&\quad - \gamma_0^{-1} \|S_\zeta^T(\hat{x}, u^*) \tilde{W}_\zeta\|) - \tilde{W}_u^T (\theta_2 \tilde{W}_u \\
&\quad - c_{\Lambda 1} \|S_u(Z_u)\| \cdot \|\tilde{x}\| - \sigma_u \|W_u^*\|) \\
&\quad - \sigma_u \tilde{W}_u^T \tilde{W}_u + \theta_2 \tilde{W}_u^T \tilde{W}_u - K e_s^2 + \theta_1 e_s^2, \tag{74}
\end{aligned}$$

where $\theta_1 > 0$ and $\theta_2 > 0$.

It can be seen that $\dot{V}_s < 0$ if e_s or \tilde{W}_u satisfies

$$\Omega_{e_s} = \{e_s : \|e_s\| \geq c_2/K\}, \tag{75}$$

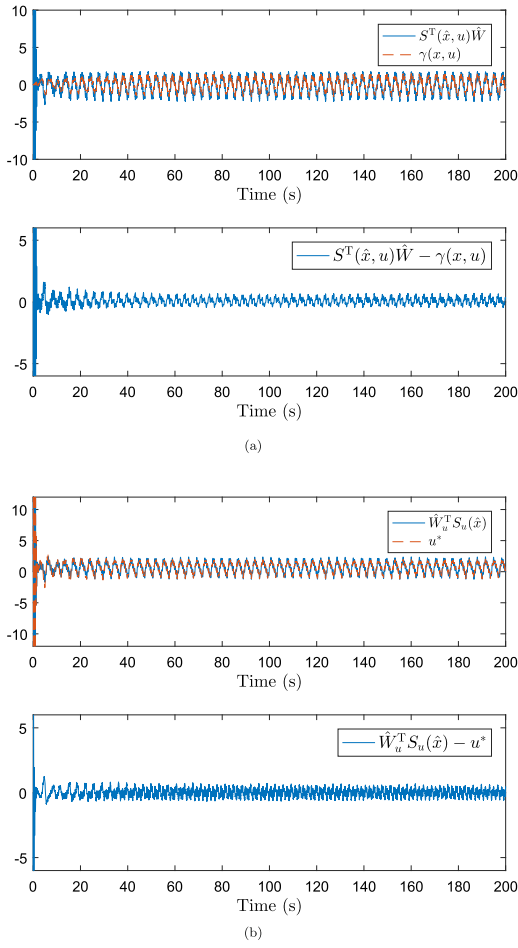


Fig. 3 The approximations of the unknown function $\gamma(x, u)$ and u^*

$$\Omega_{\tilde{W}_u} = \{ \tilde{W}_u : \|\tilde{W}_u\| \geq c_3/\sigma_u \}, \quad (76)$$

where $c_2 = (\gamma_0^{-1}c_{\Lambda 2}\|\tilde{x}\| + k_{\Lambda 1}\|\tilde{x}\| + \|\epsilon_u(Z_u)\| + \gamma_0^{-1}k_\gamma\|\tilde{x}\| + \gamma_0^{-1}\|S_\zeta^T(\hat{x}, u^*)\tilde{W}_\zeta\|)$ and $c_3 = (c_{\Lambda 1}\|S_u(Z_u)\| \cdot \|\tilde{x}\| + \sigma_u\|W_u^*\|)$.

Choose $\theta_1 = c_2/\|e_s\|$, we have determined that there is a positive correlation between θ_1 and \tilde{x} . It is evident that as the value of \tilde{x} decreases, θ_1 also decreases. This implies that the convergence speed of e_s becomes faster, and the convergence accuracy of e_s becomes higher. It can be inferred that the factor (PE level) affects the convergence speed and accuracy of \tilde{x} , and also affects the control accuracy and speed in the same manner. This ends the proof. \square

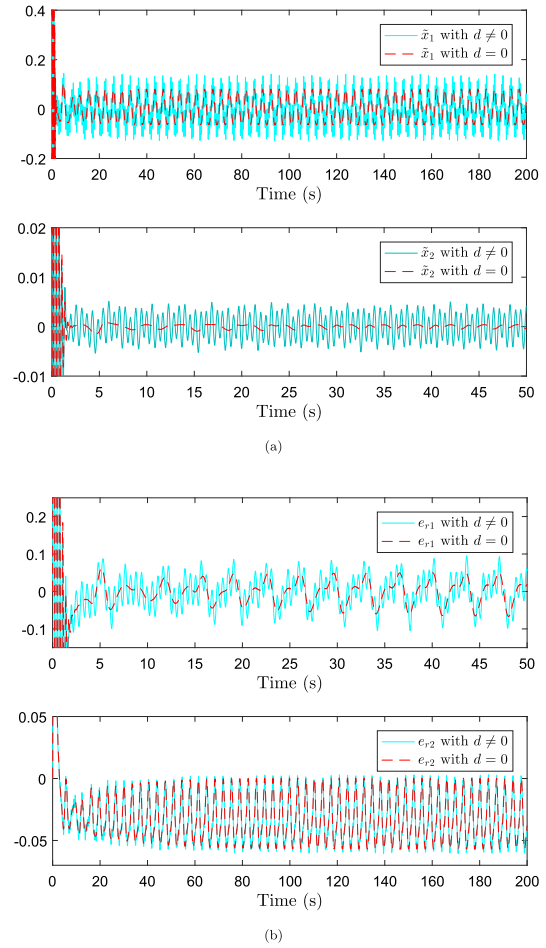


Fig. 4 State estimation error and tracking error under $d \neq 0$ and $d = 0$

Through constructing the connection between the performance of the observer and the controller, we can also conclude the relationship between the PE level of the regressor subvector of observer NN and the control speed and accuracy of the controller. Through this connection, the desired control performance can be obtained by setting the appropriate level of PE.

Specifically, in [38], the relationship between the PE level and the structures of RBF NNs have been investigated. By appropriately choosing the structure of the RBF NNs, we can achieve the desired level of PE.

5 Simulation studies

In this part, simulation result is provided to verify the effectiveness of the developed method. Consider the

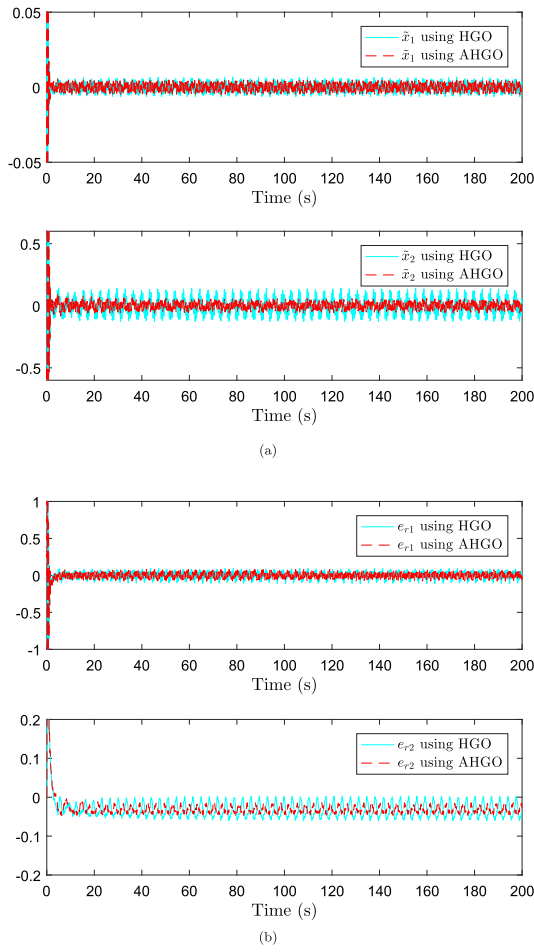


Fig. 5 State estimation error and tracking error under HGO and AHGO

following Van Der Pol oscillator as

$$\begin{aligned}\dot{x}_1 &= x_2 \\ \dot{x}_2 &= 2p_1p_2x_2 - p_1^2x_1 - 2p_1p_2p_3x_1^2x_2 + u \\ y &= x_1 + d(t)\end{aligned}\quad (77)$$

where $x \triangleq [x_1, x_2]^T$ is the system states, the measurement noise $d(t) = \sin(7t) + 3\cos(11t)/1000$, and the system parameters are set to: $p_1 = 0.9$, $p_2 = 0.6$, $p_3 = 0.95$.

The following reference system is given

$$\begin{aligned}\dot{x}_{r1} &= x_{r2} \\ \dot{x}_{r2} &= -0.4x_{r1} - x_{r1}^3 - 0.4x_{r2} + 0.62\cos(1.8t) \\ y_r &= x_{r1}\end{aligned}\quad (78)$$

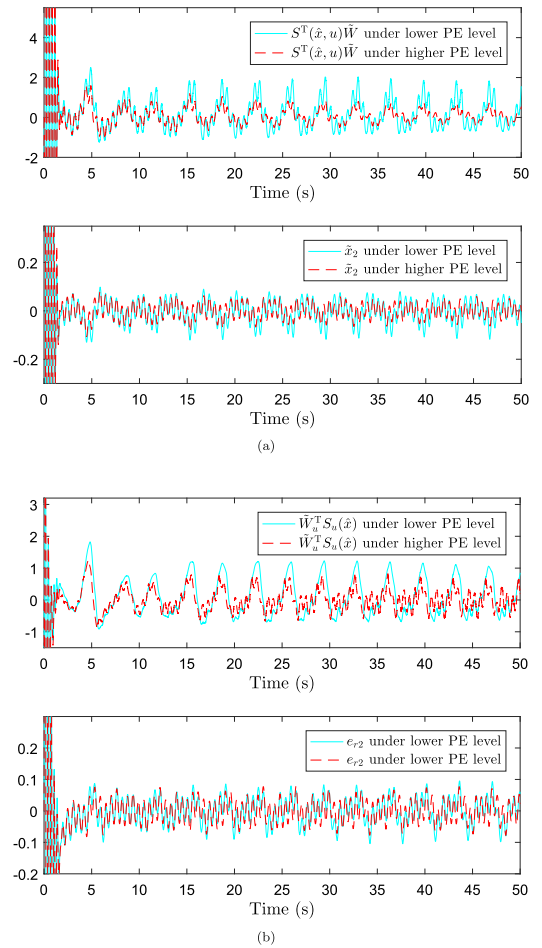


Fig. 6 State estimation error, NNs approximation error and tracking error under different value of PE level

where $x_r \triangleq [x_{r1}, x_{r2}]^T$ is the reference system states.

The observer parameters are chosen as $\rho = 35$, $\kappa_o = [1 \ 0.5]^T$ and $\Gamma = \text{diag}\{2, 2\}$, $\Omega = \text{diag}\{35, 35\}$, and $\Delta = \text{diag}\{1, 35\}$. Specifically, the nonlinear function $\gamma(x, u) = 2p_1p_2x_2 - p_1^2x_1 - 2p_1p_2p_3x_1^2x_2 + u$ is unknown. The structure of the RBF NN used to identify $\gamma(x, u)$ is as follows: nodes $N = 4$, widths $\sigma = 2$, $Z = [\hat{x}_1, u]$ and the center evenly spaced on $[-1.8, 1.8] \times [-1.8, 1.8]$.

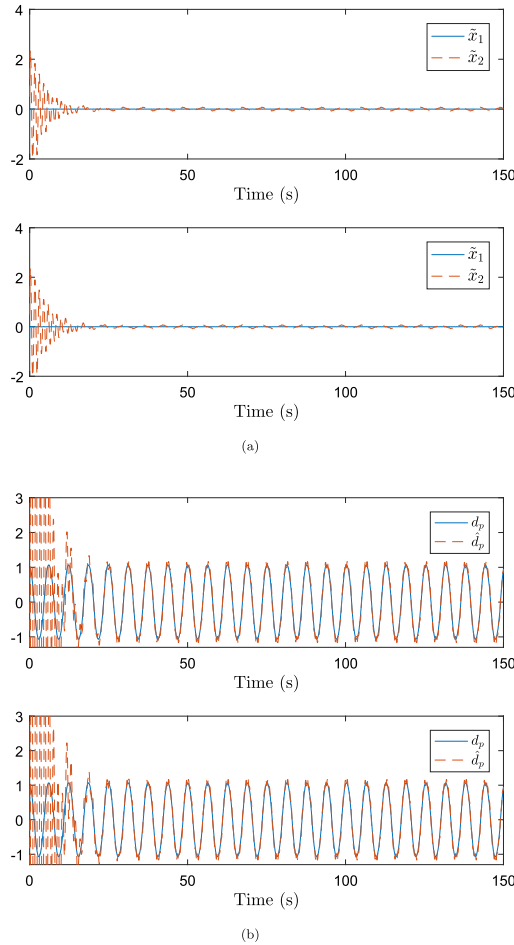
The parameters of the adaptive NN controller are designed in accordance with the controller parameters of [37] as a reference. For

$$u = -K\hat{e}_s + \hat{W}_u^T S_u(Z_u), \quad (79)$$

we design $K = 20$, and $\hat{e}_s = [1 \ 1][\hat{x}_1 - x_{r1}, \hat{x}_2 - x_{r2}]^T$. The design parameters of (69) are chosen as $\gamma_u = 0.05$

Table 1 The observer and controller performance under different values of PE level and the upper bound of PE

	Lower PE level	Higher PE level
PE level λ_1	0.0005	0.0074
The upper bound of PE λ_2	13.28	20.6337
Formula (19) λ_1/λ_2^2	3.10×10^{-6}	1.7385×10^{-5}
Max value of \tilde{x}_2 after 40s	0.1176	0.0628
Max value of e_{r2} after 40s	0.0982	0.0778
Max value of $\tilde{W}_u^T S_u(\hat{x})$ after 40s	1.8368	0.7435
Max value of $S^T(\hat{x}, u)\tilde{W}$ after 40s	1.1150	0.7889

**Fig. 7** State estimation error and the estimation of d_p by the cascade extended state observer [12]

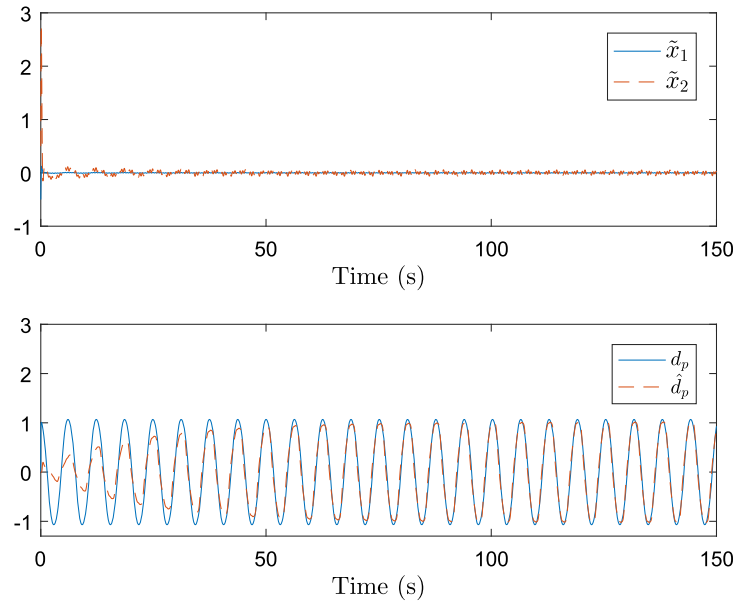
and $\sigma_u = 0.5$. Meanwhile, the RBF NN used to identify u^* is designed with 4 nodes, widths $\sigma = 1$, $Z_u = [\hat{x}_1, \hat{x}_2]$, and the center evenly spaced on $[-1.5, 1.5] \times [-1.5, 1.5]$.

Figure 1 illustrates that accurate state estimations of x_1 and x_2 are obtained, and the state estimation errors converge close to zero. The tracking performance is depicted in Fig. 2. It shows that the state x can track the desired signal x_r quickly and accurately. The identifications of $\gamma(x, u)$ and u^* are shown in Fig. 3. It shows that the RBF NNs $S^T(\hat{x}_1, u)\tilde{W}$ and $\tilde{W}_u^T S_u(\hat{x}_1, \hat{x}_2)$ can approximate $\gamma(x, u)$ and u^* , respectively. Meanwhile, the approximation errors converge to converge to a small neighborhood of zero. Two situations with or without noise are compared in Fig. 4. It indicates that the proposed method can maintain a certain level of state estimation and tracking capability even in the presence of measurement noise. A standard high gain observer (HGO) is employed to verify the superiority of the proposed adaptive NN method. Figure 5 shows that both HGO and AHGO can obtain the accurate state estimations under the same gain, but the estimation speed and accuracy of the AHGO are higher.

By modifying the structure of the RBF NN, we can achieve different values of λ_1 and λ_2 , allowing us to assess the performance of the observer and controller under these circumstances. It is important to note that it is typically challenging to independently increase the PE level λ_1 while keeping the upper bound unchanged. Therefore, according to formula (57), we must ensure that the value of λ_1/λ_2^2 also increases when increasing the PE level λ_1 .

To facilitate observation, we selected a subset of states that exhibit significant changes. From Fig. 6, we can see that when the PE level is relatively high, the estimation accuracy and speed regarding unknown dynamics improve, leading to enhanced observer performance. Figure 6b indicates a positive correlation between a higher PE level and controller performance.

Fig. 8 State estimation error and the estimation of d_p by using the AHGO



Detailed parameters and accuracy for Fig. 6 are displayed in Table 1.

Next, we will compare our approach with the method proposed in [12], a cascade extended state observer with two levels is designed to estimate the states of system (77). We change the system dynamics as $\dot{x}_2 = 2p_1p_2x_2 - p_1^2x_1 - 2p_1p_2p_3x_1^2x_2 + u + d_p$, where $\gamma(x, u) = 2p_1p_2x_2 - p_1^2x_1 - 2p_1p_2p_3x_1^2x_2 + u$ is known, $d_p = d_t + d_x$, in which $d_t = 0.2 \cos(t)$ is the process noise, and $d_x = 0.2x_2 + \sin(x_1)$ is unknown system dynamics. Here, we primarily compare the performance of the two observers. Typically, u does not affect the performance of the observer; therefore, we let output y tracks $y_r = \cos(t)$ by designing the control input u with the aid of the backstepping method.

Figure 7 shows the performance of the 1 level and 2 level cascade extended state observer, while Fig. 8 presents the performance of the AHGO. From Figs. 7–8, it can be seen that both observers can estimate the system states in the presence of measurement noise, the process noise, and unknown system dynamics. Specifically, the cascade extended state observer can estimate states and d_p rapidly, but the estimation curves of x_2 and d_p (curve \hat{d}_p) is not as smooth as that of the AHGO. This may necessitate the addition of more cascade layers to improve estimation accuracy while minimizing the impact of measurement noise. In contrast, the method presented in this paper is simple design and application, leveraging the learning capability of NN to

achieve better estimation of d_p , which in turn leads to accurate estimation of x_2 .

6 Conclusion

In this paper, we explore an AHGO-based adaptive NN control method for a class of nonlinear systems via the DLM. Initially, an AHGO is utilized to reconstruct the system states. By employing the DLM, the subvectors associated with the NNs satisfy the partial PE condition, and then the unknown dynamics can be approximated accurately. The convergence characteristics of the error system are analyzed, revealing a direct relationship between the learning speed and estimation accuracy with the level and the upper bound of PE. Subsequently, through a suitable state transformation and utilizing the reconstructed states as feedback signals, an adaptive NN controller is employed to acquire knowledge and stabilize the nonlinear systems. The convergence characteristics of the closed-loop systems are also analyzed, and we find that the control performance is influenced by the observer's performance. This implies that the PE level of the regressor subvector of the observer NN also impacts the convergence speed and accuracy of the controller. Consequently, a higher level of PE can ensure faster control speed and higher control accuracy. The significance of this article lies in revealing that the convergence performance of closed-

loop systems is not only affected by the observer and control gains, but also by the level of PE of the regressor subvector of the observer NN. Simulation examples are provided to demonstrate the effectiveness of the proposed method.

Acknowledgements This work was supported by the Natural Science Foundation of Shandong Province (ZR2022MF301).

Funding This work was supported by the Natural Science Foundation of Shandong Province (ZR2022MF301).

Data availability No data was used for the research described in the article.

Declarations

Conflict of interest The authors declare that they have no known competing financial interests or personal relationships that could have appeared to influence the work reported in this paper.

Declaration of generative AI in scientific writing The generative artificial intelligence (AI) and AI-assisted technologies have only used in this paper to improve readability and language, and not to the use of AI tools to analyse and draw insights from data as part of the research process.

References

- Hu, J., Wu, W., Ji, B., Wang, C.: Observer design for sampled-data systems via deterministic learning. *IEEE Trans. Neural Netw. Learn. Syst.* **33**(7), 2931–2939 (2021)
- Hu, J., Wu, W., Zhang, F., Wang, C.: Learning from output-feedback control of sampled-data systems in normal form. *IET Control Theory Appl.* **18**(3), 265–278 (2024)
- Bernard, P., Andrieu, V., Astolfi, D.: Observer design for continuous-time dynamical systems. *Annu. Rev. Control.* **53**, 224–248 (2022)
- Shakarami, M., Esfandiari, K., Suratgar, A.A., Talebi, H.A.: Peaking attenuation of high-gain observers using adaptive techniques: state estimation and feedback control. *IEEE Trans. Autom. Control* **65**(10), 4215–4229 (2020)
- Adil, A., Zemouche, A., Hamaz, A., Laleg-Kirati, T.M., N'Doye, I., Bedouhene, F.: High-gain observer design for nonlinear systems with delayed outputs. *IFAC-PapersOnLine* **53**(2), 5057–5062 (2020)
- Lin, Z.: Co-design of linear low-and-high gain feedback and high gain observer for suppression of effects of peaking on semi-global stabilization. *Automatica* **137**, 110124 (2022)
- Wang, L., Astolfi, D., Marconi, L., Su, H.: High-gain observers with limited gain power for systems with observability canonical form. *Automatica* **75**, 16–23 (2017)
- Prasov, A.A., Khalil, H.K.: A nonlinear high-gain observer for systems with measurement noise in a feedback control framework. *IEEE Trans. Autom. Control* **58**(3), 569–580 (2012)
- Zemouche, A., Zhang, F., Mazenc, F., Rajamani, R.: High-gain nonlinear observer with lower tuning parameter. *IEEE Trans. Autom. Control* **64**(8), 3194–3209 (2018)
- Busawon, K.K., Kabore, P.: Disturbance attenuation using proportional integral observers. *Int. J. Control.* **74**(6), 618–627 (2001)
- Khalil, H.K., Priess, S.: Analysis of the use of low-pass filters with high-gain observers. *IFAC-PapersOnLine* **49**(18), 488–492 (2016)
- Lakomy, K., Madonski, R.: Cascade extended state observer for active disturbance rejection control applications under measurement noise. *ISA Trans.* **109**, 1–10 (2021)
- Chen, T., Zeng, C., Wang, C.: Fault identification for a class of nonlinear systems of canonical form via deterministic learning. *IEEE Trans. Cybern.* **52**(10), 10957–10968 (2021)
- Xu, A., Zhang, Q.: Nonlinear system fault diagnosis based on adaptive estimation. *Automatica* **40**(7), 1181–1193 (2004)
- Zhang, Q., Besançon, G.: Nonlinear system sensor fault estimation. *IFAC Proc. Vol.* **38**(1), 107–112 (2005)
- Farza, M., M'Saad, M., Maatoug, T., Kamoun, M.: Adaptive observers for nonlinearly parameterized class of nonlinear systems. *Automatica* **45**(10), 2292–2299 (2009)
- Guo, C., Hu, J.: Fixed-time stabilization of high-order uncertain nonlinear systems: Output feedback control design and settling time analysis. *J. Syst. Sci. Complex.* 1–22 (2023)
- Tang, H., Zhang, T., Xia, M.: Command filter and high gain observer based adaptive output feedback control for stochastic nonlinear systems with prescribed performance and input quantization. *Int. J. Adapt. Control Signal Process.* (2023). <https://doi.org/10.1002/acs.3726>
- Yoo, S.J., Park, B.S.: Prescribed-time adaptive state observer approach for distributed output-feedback formation tracking of networked uncertain underactuated surface vehicles. *Nonlinear Dyn.* 1–16 (2024)
- Han, Q., Liu, Z., Su, H., Liu, X.: Filter-based adaptive backstepping attitude control for multi-rotor uavs with parametric uncertainty, external disturbance and input saturation. *Nonlinear Dynamics* pp. 1–18 (2024)
- Jing, C., Zhang, H., Yan, B., Hui, Y., Xu, H.: State and disturbance observer based robust disturbance rejection control for friction electro-hydraulic load simulator. *Nonlinear Dyn.* 1–15 (2024)
- Li, S., Ahn, C.K., Guo, J., Xiang, Z.: Neural-network approximation-based adaptive periodic event-triggered output-feedback control of switched nonlinear systems. *IEEE Trans. Cybern.* **51**(8), 4011–4020 (2020)
- Ma, L., Xu, N., Zhao, X., Zong, G., Huo, X.: Small-gain technique-based adaptive neural output-feedback fault-tolerant control of switched nonlinear systems with unmodeled dynamics. *IEEE Trans. Syst. Man Cybern. Syst.* **51**(11), 7051–7062 (2020)
- Wang, H., Liu, S., Yang, X.: Adaptive neural control for non-strict-feedback nonlinear systems with input delay. *Inf. Sci.* **514**, 605–616 (2020)
- Kong, J., Niu, B., Wang, Z., Zhao, P., Qi, W.: Adaptive output-feedback neural tracking control for uncertain switched mimo nonlinear systems with time delays. *Int. J. Syst. Sci.* **52**(13), 2813–2830 (2021)

26. Yan, L., Ma, B., Jia, Y.: Trajectory tracking control of non-holonomic wheeled mobile robots using only measurements for position and velocity. *Automatica* **159**, 111374 (2024)
27. Wang, C., Hill, D.J.: Deterministic Learning Theory for Identification, Recognition, and Control. CRC Press, London (2018)
28. Yuan, C., Wang, C.: Persistency of excitation and performance of deterministic learning. *Syst. Control Lett.* **60**(12), 952–959 (2011)
29. Zeng, Y., Chen, T., Wang, C.: Fault diagnosis for a class of nonlinear uncertain systems using deterministic learning approach. *J. Franklin Inst.* **360**(8), 5609–5633 (2023)
30. He, K., Dong, C., Wang, Q.: Active disturbance rejection control for uncertain nonlinear systems with sporadic measurements. *IEEE/CAC J. Autom. Sin.* **9**(5), 893–906 (2022)
31. Khalil, H.K.: Nonlinear Control. Pearson, New York (2015)
32. Shil'nikov, L.P.: Methods of Qualitative Theory in Nonlinear Dynamics, vol. 5. World Scientific, Singapore (2001)
33. Sastry, S., Bodson, M., Bartram, J.F.: Adaptive Control: Stability, Convergence, and Robustness (1990)
34. Ioannou, P.A., Sun, J.: Robust Adaptive Control. Courier Corporation, New York (2012)
35. Vamvoudakis, K.G., Lewis, F.L.: Online actor-critic algorithm to solve the continuous-time infinite horizon optimal control problem. *Automatica* **46**(5), 878–888 (2010)
36. Park, J.H., Kim, S.H., Moon, C.J.: Adaptive neural control for strict-feedback nonlinear systems without backstepping. *IEEE Trans. Neural Netw.* **20**(7), 1204–1209 (2009)
37. Dai, S.L., Wang, C., Wang, M.: Dynamic learning from adaptive neural network control of a class of nonaffine nonlinear systems. *IEEE Trans. Neural Netw. Learn. Syst.* **25**(1), 111–123 (2013)
38. Zheng, T., Wang, C.: Relationship between persistent excitation levels and rbf network structures, with application to performance analysis of deterministic learning. *IEEE Trans. Cybern.* **47**(10), 3380–3392 (2017)

Publisher's Note Springer Nature remains neutral with regard to jurisdictional claims in published maps and institutional affiliations.

Springer Nature or its licensor (e.g. a society or other partner) holds exclusive rights to this article under a publishing agreement with the author(s) or other rightsholder(s); author self-archiving of the accepted manuscript version of this article is solely governed by the terms of such publishing agreement and applicable law.